EUROPEAN ORGANIZATION FOR NUCLEAR RESEARCH

CERN/SPSC/81-14
SPSC/P 158
13 February 1981

PROPOSAL

SEARCH FOR NEUTRINO OSCILLATIONS IN THE SPS WIDE-BAND BEAM

CERN: A. Grant

Imperial College: T.C. Bacon, I. Butterworth, W. Cameron

Oxford: G. Myatt, D. Radojičić, B. Saitta

Annecy: M. Steuer, F. Vannucci

We propose to search for neutrino oscillations in the SPS wide-band beam by measuring the disappearance of ν_μ events and the appearance of ν_e and ν_τ events. This is done by comparing the ratios of neutral-current to charged-current events, and of events with electrons to events with muons. It is stressed that the best method uses quasielastic events. Two detectors are needed, one positioned close to the production target, the other one 17 km away from it. The two detectors have the same structure and are composed of a fine-sampling calorimeter using flash-tubes followed by a magnetized iron spectrometer.

G E N E V A
1981

1. INTRODUCTION

Neutrino oscillations were first proposed many years ago[1]. They have recently become topical with the publication of results suggesting that neutrinos may have a non-zero mass:

i) a finite mass is claimed for the ν_e in a study of the endpoint in the spectrum of the β decay of tritium[2];

ii) a ratio of charged-current to neutral-current cross-sections induced by $\bar{\nu}_e$ at a reactor is interpreted as evidence for neutrino instability[3];

iii) a beam-dump experiment at CERN yields significantly more muons than electrons[4].

These results do not give a satisfactory understanding of the phenomenon, and the existence of neutrino oscillations[5] is not yet demonstrated.

Here we propose an experiment which is an order of magnitude more sensitive than any proposed so far, and which is sensitive to the possibility of three-way mixing between neutrino types.

On the theoretical front, developments in grand unified theories (GUTs) tend to favour the mixing of neutrino species, and they generally predict masses in the range[6]:

$$10^{-5} < M_\nu < 1.0 \text{ eV} .$$

This is only possible in theories which go beyond SU(2) × U(1). As a consequence, the discovery of neutrino oscillations would be a first sign of what happens beyond the mass scale of 100 GeV, which is appropriate for the present electroweak models.

By analogy with the Kobayashi-Maskawa mixing matrix among quarks, it has been argued that the dominant mixing could be between ν_μ and ν_τ [7]. It suggests that the oscillation $\nu_\mu \leftrightarrow \nu_\tau$ could be the most probable.

Even with massless ν's there is the possibility of oscillation in matter[8], although present estimates give little hope of experimental detection. Other considerations relevant to this experiment are: the possibility of $\nu \rightarrow \bar{\nu}$ oscillations[9], and the occurrence of CP violations in the process[10].

2. MEASURING NEUTRINO OSCILLATIONS

2.1 Probability of oscillation

For the sake of simplicity, we discuss the sensitivity of this experiment assuming mixing between two states. The probability of oscillation between two neutrinos ν and ν' is given by

$$P_{\nu \to \nu'} = \frac{1}{2} \sin^2 2\theta \left(1 - \cos 2\pi \frac{R}{L}\right) = \sin^2 2\theta \sin^2 \pi \frac{R}{L} ,$$

where R is the distance between production and observation, θ is the mixing angle between the two neutrinos, and L is the oscillation length:

$$L = 2.5 \frac{E \text{ (GeV)}}{\Delta m^2 \text{ (eV}^2\text{)}} \quad \text{(km)} ,$$

where $\Delta m^2 = |m^2_{\nu_1} - m^2_{\nu_2}|$, with ν_1 and ν_2 referring to the neutrino mass eigenstates.

Present limits come from the Gargamelle bubble chamber[11] for $\nu_\mu \to \nu_e$ and $\bar{\nu}_\mu \to \bar{\nu}_e$, from LAMPF[12] for $\nu_\mu \to \nu_e$, and from FNAL[13] for $\nu_\mu \to \nu_e$ and $\nu_\mu \to \nu_\tau$. They can be compared by assuming maximum mixing ($\sin^2 2\theta = 1$). The limit for Δm^2 is about 1 eV^2 from all three experiments. A new experiment at Grenoble[14] claims the very good limit $\Delta m^2 < 0.15$ for the transition $\bar{\nu}_e \to \nu'$.

If the mixing is indeed not very small, the oscillation length must be large, and experiments at accelerators are testing oscillations in a range of distances for which $R/L \ll 1$. In this case the probability of detecting an effect increases like $(R/L)^2 \propto (R/E)^2$. Consequently, an experiment should try to maximize R/E by choosing either low neutrino energies or long distances. We will argue in favour of the second solution. Similar considerations have already been discussed elsewhere[15].

2.2 Advantages of high energy

We propose to use the SPS wide-band beam for the following reasons:

- As emphasized in our Letter of Intent, SPSC/I135, the rates of detected events in a given detector are more favourable, essentially because the neutrino cross-section rises linearly with energy.
- The background from cosmic events, very difficult to handle for a few 100 MeV beam, is here easy to reject both in energy deposition and in directionality.
- The contamination of the initial beam in ν_e, which dictates the present limit of the FNAL search, is smaller at long distances because of the larger divergence of the ν_e beam produced in K_{e3} decays.
- The identification of muons by penetration is very easy at high energies, and the energy resolution for electron and hadron showers, using calorimetry techniques, improves with energy.
- Finally, the ν_τ is no longer sterile, being well above threshold for τ production. Should oscillations be found, it is conceivable that this is the best way to investigate ν_τ interactions.

2.3 Principle of the measurement

To detect a change in the composition of a ν beam, it is essential to have (at least) two measuring stations at two different places along the beam. Measurements with only one detector have to rely on calculated fluxes that are prone to systematic errors. On the contrary, measuring neutrino interactions simultaneously in two detectors allows a comparison that is immune to beam changes and, to a good approximation, is independent of the beam spectrum. It is safest to use two detectors with the same longitudinal structure so as to avoid biases resulting from acceptance corrections. The comparison will be made between positively identified classes of events: charged current (CC) ν_μ, ν_e, and ν_τ events; neutral current (NC) events; with the same cuts applied to both detectors to define these classes.

2.4 A detector in the Jura

Looking for oscillations in a high-energy neutrino beam necessitates long distances between the two detecting stations. The first detector (detector 1) could be housed in the Gargamelle hall (940 m from the target). The second one (detector 2) has to be positioned at the furthest practical distance. Figure 1 shows the neutrino wide-band beam across the profile of the Jura mountain. The beam re-emerges at a distance of 17.5 km in the "forêt communale de Cernétrou". This place is easy to reach, being near a road. The position is known to 1 m (see Appendix 1). This is well within the natural divergence of the beam, which will be more than 10 m at this distance. The direction of the incident proton beam is stable to better than 0.02 mrad, and such small instabilities would give negligible variations at the level of the detector.

3. THE BEAM

Two beams have been considered: the standard wide-band beam currently operated, and one designed to maximize the event rate between 10 and 30 GeV by reducing the distance between target and horn. In each case 450 GeV operation has been assumed. Since the optimized beam gives significantly greater sensitivity we prefer this option, and figures have been calculated on this basis. However, we also give the results for the standard beam.

3.1 Neutrino flux at 17 km

The flux hitting a detector 17 km from the production target was computed by the standard wide-band beam program, with simulations of K^+, π^+, K^0, and Λ^0 decays. The results are presented in Table 1 for both the standard and optimized beams for 10^{13} protons on target. Figure 2 shows the spectra in the optimized case. Contaminations from other neutrino species are as follows:

$$\nu_e = 5.0 \times 10^{-3}$$
$$\bar{\nu}_\mu = 3.4 \times 10^{-3}$$
$$\bar{\nu}_e = 6.2 \times 10^{-4} \ .$$

These contaminations, and in particular the ν_e beam, have spectra that are very different from the dominant ν_μ beam, as may be seen from Fig. 2.

In order to study the sensitivity of the beam to a sideways shift, the flux has also been calculated for a detector positioned 5 m off axis. There is no significant change in the spectrum or the contamination intensities.

3.2 Matching the solid angles

In comparing neutrino fluxes in two detectors it is essential to understand the possible systematic effects which can affect the result. The extended neutrino source is such an effect. Ideally we would like the two detectors to match the same solid angle. This is only possible with a point-like source. Here the source is 300 m long and 1.2 m wide. If we define the transverse dimensions of the two detectors such that they see the same solid angle for a point-like emission set in the middle of the decay path, then the corrections can be readily computed. We find that the solid angle seen by the first detector is 3% larger than the second one, owing to the length and the lateral extension of the ν source.

These two geometrical corrections, which depend only on geometrical dimensions, can be accurately determined and the fluxes corrected.

3.3 The spectrum in the closer detector

Because of the non-point-like source, the closer detector sees neutrinos emitted at a larger decay angle, and the spectrum may be softer than in the far-away detector for which the beam is almost parallel. This is shown in Fig. 3, where the spectra in the two detectors are compared. Thus although the two detectors can be chosen such that the fluxes traversing them are equal, because of the different spectra the number of ν events in detector 1 will be smaller than in detector 2.

3.4 Sensitivity to beam properties

To overcome the difficulty of the different spectra, we therefore propose to compare ratios of NC to CC ν events in the two detectors. For a given ν species this ratio is independent of the spectrum. If there is oscillation the spectrum does not change, and the NC events are unaffected since all ν of a given momentum will give the same NC event in a detector. Thus the disappearance of ν_μ between detector 1 and detector 2 will be measured by comparing the ratio of NC to CC ν_μ events in the two detectors. This method of comparing ratios also avoids the

necessity of knowing precisely the dimensions of the detectors, which otherwise give systematics at a level of a few percent.

The appearance of ν_e (ν_τ) will be measured by comparing the ratio of CC ν_e (CC ν_τ) to CC ν_μ events. It is then essential to have detectors that can make the best possible identification of both muons and electrons in the final state.

4. THE TWO DETECTORS

The detectors must be able to identify electrons and muons. Furthermore, they must give a measurement of muon momentum and of electron and hadron energies. They will be composed of two parts: a fine-sampling calorimeter which is also the target, followed by a muon spectrometer.

4.1 Dimensions of the detector

In order to collect a large sample of events, we propose to use a target of 100 tons fiducial volume for the larger detector. This will then have the dimensions $3.4 \times 3.4 \times 1.1$ m^3 of equivalent iron. As we want to measure the energy of the events, the detector must contain the shower development. It will be argued that, for the main measurement, we need contain only the electromagnetic shower. For this purpose the final dimensions will be $3.7 \times 3.7 \times 1.5$ m^3 of equivalent iron. However, it is probably desirable to precede the detector by 50 cm of active neutron shield made up of 10 cm iron slabs interspersed with flash-tubes.

The small detector has transverse dimensions scaled down from the big one, and the same longitudinal dimensions. The dimensions, after provision for containment, will be approximately

$$1.5 \times 1.5 \times 1.5 \text{ m}^3 \ .$$

4.2 The electron calorimeter

In order to recognize electrons produced together with hadrons, the calorimeter has to have a fine grain. It will be composed of a stack of 3 mm thick iron plates and flash-tube planes[16]. These planes, which are commercially available, are made of black polypropylene. They are 5.5 mm thick with rectangular holes of 4.5×5 mm^2. A mixture of neon-helium at atmospheric pressure circulates in them. The electric field necessary for the development of the plasma is applied to aluminium layers, 60 μm thick, glued on the plastic. Two planes of flash-tube are paired together with the high-voltage layer in between. Figure 4 shows the detail of one cell of the calorimeter with an iron plate and a bigap of flash-tube planes. Figure 5 shows the resulting resolution for EM showers.

Each target will be made of 500 such cells for a total of 1.5 m of iron. This requires 336,000 channels for detector 2 and 136,000 channels for detector 1.

4.3 Tests of large-size flash planes

Long flash-tubes of length 5.5 m have been tested at Saclay using a gas mixture NEOGAL 70 (70% neon, 30% helium). The high-voltage pulse was provided by a delay-line cut in an aluminium foil insulated from a ground plate by a mylar sheet[17]. This arrangement is shown in Fig. 4. It gives a high-voltage pulse of rectangular shape and width 200 ns which is sufficient for the plasma to propagate along the tube length. The plasma reaching the end of the tube emits a visible light which can be photographed. Figure 6 shows the test set-up and an example of cosmic-rays traversing a stack of 10 planes. The efficiency of detection per plane is shown in Fig. 7. It reaches 80% at $\sim$ 8 kV with a plateau of 2 kV, and is independent of the particle position along the tube. The number of random hits is also shown in Fig. 7. These hits originate from photons produced in an excited tube being reflected at the window into other tubes. These accidentals decrease when the back-window is blackened, and should be very small with an electronic read-out which does not require a window.

The read-out is being developed at Wuppertal. In principle, as there is sufficient charge picked up by the pins inserted into the plasma to flip a shift register without amplification, a very simple and cheap read-out can be built. Prototypes built at Wuppertal have shown that this is possible and the estimated price for the complete system up to the computer interface has been costed at 1 SFr per channel.

4.4 The muon spectrometer

This follows the target-calorimeter and provides a filter to absorb the hadrons together with a magnetic field to momentum analyse muons. It can also be used as a target to increase the sample of μ events for the $\nu_\mu \rightarrow \bar{\nu}_\mu$ oscillation search. The spectrometer for detector 2 uses three dipolar magnets of dimensions $3.7 \times 3.7 \times 0.5$ m^3 each. The field produced by coils wound through holes 2 m $\times$ 30 mm is shown in Fig. 8. It reaches 16.8 kG. No water-cooling is necessary and the power consumption is low: 4 kW per magnet. All the iron is available from the now completed R209 dimuon experiment at the ISR. The magnet for detector 1 will be a scaled down version of the one for detector 2.

The drift chambers are assembled in modules of x-x-y-y planes. We need a total of six modules containing 900 wires. With a spatial resolution of 500 μm per wire, the initial and final direction of the muons can be measured with an error of 1 mrad. The momentum resolution, taking into account multiple scattering and measurement resolution, is shown in Fig. 9.

The efficiency of identification as a function of muon momentum is shown in Fig. 10. It should be remembered that this will be the same in both detectors and therefore does not enter directly into the detection of oscillation.

4.5 The trigger system

A trigger is required to pulse the high voltage of the flash-tube system. Also the dead-time being of the order of 1 s it is essential not to trigger on cosmic-ray events. To achieve this, a system of hodoscopes of scintillator counters is used. To be fully efficient on real events having an electron, the planes of counters must be separated by less than the extension of an electromagnetic shower. Figure 11 shows the trigger efficiency for electrons. It is sufficient to have one plane every 30 cells of iron flash-tubes, namely every 5.0 radiation lengths of iron. Each of the hodoscopes will be composed of nine elements 3.6 m long and 40 cm wide. Two-inch phototubes will detect the light at both ends, allowing a 50 cm spatial resolution along the counters. The trigger will require the coincidence of counters of adjacent scintillator planes.

Figure 12 shows the over-all view of detector 2. The total lengths are 7 m for the calorimeter and 2.7 m for the muon spectrometer. The target is subdivided into 16 modules of 30 cells each, separated by scintillator hodoscopes. As previously discussed, the target is preceded by an active neutron absorber.

5. PERFORMANCES

5.1 Event rate

The total number of CC ν_μ events produced for 10^{19} protons and a 100 ton target is 32,000 in the case of the optimized beam. Of these events 18,750 correspond to a neutrino energy between 10 and 30 GeV. Comparison of event rates between standard and optimized beams is given in Table 1. During a 1 ms long spill, a few cosmics traverse the detector, and the probability of a beam ν_μ event generated in the target is 0.04. Thus a selective trigger is required. Another category of events will generate possible triggers: these are the ν_μ events produced in the mountain in front of the detector. A Monte Carlo study gives a probability of seeing two such events per pulse in the detector. These events are easily identified by TOF between the front and the back layers of scintillators. They can be used to calibrate the detector and also to check the timing of the beam gate. It is foreseen that a cheap form of leased cable can be used to transmit timing information to the remote site.

5.2 Monte Carlo program

In order to estimate the ability of an iron flash-tube calorimeter to identify the different categories of ν events, a simulation of the detector has been

developed. Real CC ν_μ events have been generated, and in some cases the muon has been replaced either by an unseen neutrino or by an electron. A total of 100 events has been produced with the actual spectrum of the ν beam. Figure 13 shows some characteristic events: CC ν_μ event (Fig. 13a), NC event (Fig. 13b), and a CC ν_e event (Fig. 13c).

The CC ν_μ events are unambiguous for muon momenta above 2 GeV (90% of the CC ν_μ events). Discrimination between NC events and CC ν_e events is more difficult because electromagnetic showers can be masked by hadronic showers. More studies have to be made, especially with actual data. Here we argue that there is a method, less prone to systematic errors, for measuring the ratio ν_e/ν_μ: the study of quasi-elastic charged current (QECC) events, i.e. $\nu_\mu n \to \mu^- p$, $\nu_e n \to e^- p$, and $\nu_\tau n \to \tau^- p$. These channels account for several percent of the total cross-section. Because of their y distribution they are very easily identifiable and the final lepton gives a good estimate of the initial neutrino energy. The detector is very well suited for this purpose: Fig. 14 shows examples of quasi-elastic events. This method allows a sure containment of the hadron energy.

5.3 Sensitivity to oscillations

With 10^{19} protons on target we could accumulate 32,000 CC ν_μ events and 10,700 NC ν_μ events in each of the two detectors. In practice, QECC events will be defined by hadron energy less than 1.5 GeV, for which the cross-section is estimated to be 2.5×10^{-38} cm^2/nucleon, independent of energy above a threshold of $\sim$ 1.5 GeV. With 10^{19} protons on target this gives QECC ν_μ events, among which 4000 have an energy between 10 and 30 GeV. The spectrum of the electrons produced in QECC ν_e events arising from a possible oscillation and of the muons produced in QECC ν_μ events will be the same. This allows a check on any effect observed.

With these numbers in mind we can extract the sensitivity of this experiment to search for oscillations:

a) The disappearance of ν_μ can be detected by comparing the ratio NC/CC, where CC includes all events with a well-reconstructed muon, and NC is the remainder. The comparison of ratios will be independent of uncertainties in the relative size of the detectors. Without oscillation the ratio NC/CC is independent of energy, thus independent of a difference of spectra in detector 1 and detector 2. A possible error comes from the evaluation of the number of CC ν_μ events where the muon is not identified. The proportion of such events is small (5%) and a correction can be estimated to within 10%. Other backgrounds such as $\pi, K \to \mu$ decays, geometrical inefficiencies, etc., are also common to both detectors, and therefore cancel in first order in

the comparison. The active neutron shield will protect the fiducial regions from incident hadron background which could be different in the two detectors. Considering the 5400 NC events in the energy range 10 to 30 GeV, the statistics limit the comparison of the ratios NC/CC in the two detectors to 1.9%. This translates into the limit: $\sin 2\theta\ \Delta m^2 < 0.15\ eV^2$ (90% C.L.).

b) The appearance of ν_e and ν_τ is searched for in the QECC events. Background for the process $\nu_e n \to e^- p$ comes first from the initial ν_e contamination, which will give 15 events in both detectors in the range 10 to 30 GeV. As the electron carries the ν energy information, it is possible to reject some fraction of these background events because of the difference between the ν_μ and ν_e spectra. Another background comes from $\nu_\mu e$ scattering. The expected number of such events is 10, with equal contributions in detectors 1 and 2. Finally there is the possibility of NC events with fast π^0 in the final state. From BEBC results[18] we evaluate the probability of having a fast π^0 in NC quasi-elastic events to be 6.5%. This gives 75 such events in our sample. The upper limit on the probability of a π^0 faking an electron is estimated to be 40%. This gives a maximum of 30 events. Again this background is the same in the two detectors. The comparison of rates in the two detectors gives an upper limit on ν_e/ν_μ of less than 4×10^{-3}. This gives a limit for the oscillation $\nu_\mu \to \nu_e$ of: $\sin 2\theta\ \Delta m^2 < 0.06\ eV^2$ (90% C.L.).

c) The signal for the oscillation $\nu_\mu \to \nu_\tau$ will also be obtained by the study of quasi-elastic events: the signature for τ decay will be an electron, emitted at large transverse momentum. With a branching ratio $\tau \to e\nu\bar{\nu}$ of 17% and a 30% loss due to threshold effects in the production of CC ν_τ events, the number of background events discussed previously gives the limit: $\sin 2\theta\ \Delta m^2 < 0.13\ eV^2$ (90% C.L.).

The limits expressed in terms of Δm^2 and $\sin^2 2\theta$ are shown in Fig. 15, together with some recent results on searches for oscillations.

6. CONCLUSION

We propose a dedicated experiment to search for neutrino oscillations. This experiment improves the limit on the existence of oscillations by at least one order of magnitude. To have an idea of the sensitivity of this search, it is enough to realize that, if $\Delta m^2 = 0.15\ eV^2$ for any pair of neutrinos (corresponding to the best upper limit ever quoted), the experiment would still give rise to 830 CC events from oscillating neutrinos. For a mixing angle "à la Cabibbo", $\sin^2 2\theta \sim 0.05$, and $\Delta m^2 = 1\ eV^2$, the number of "oscillated" events is 1850.

The experiment is done with the SPS neutrino beam and need not disturb the rest of the neutrino physics program. In this proposal we have assumed the use of an optimized wide-band beam. Use of the standard beam would, for the same number of protons, lead to 20% worse limits in Δm^2, as shown in Table 1.

This experiment is the only one proposed to search for the $\nu_\mu \rightarrow \nu_\tau$ oscillation which may be favoured theoretically. Should an effect be seen, this experiment gives an opportunity for proving the existence of the ν_τ.

Costs are not high for such a potentially fundamental search and a present estimate is given in Appendix 2. In particular the demands on CERN would be small. They would consist of establishing communications and facilities to mount the experiment at a distance of 17 km in the Jura, and possibly modifying the beam. The detectors would be provided by the participating laboratories. The Saclay Group working on a proton lifetime experiment has offered the present collaboration to support this experiment in any possible way which is not incompatible with the τ_p experiment, the two detectors being very similar.

Acknowledgements

We thank A. Ball for calculating the beam spectra, and B. Tallini for many helpful discussions on the detector.

REFERENCES

1) B. Pontecorvo, Zh. Eksper. Teor. Fiz. 53 (1967) 1717.
S.M. Bilenky and B. Pontecorvo, Phys. Rep. 41 (1978) 225.

2) V.A. Lyubimov et al., Phys. Lett. 94B (1980) 266.

3) F. Reines et al., Phys. Rev. Lett. 45 (1980) 1307.

4) F. Dydak (CDHS Collaboration), Neutrino Conference, Erice, 1980.
M. Jonker et al. (CHARM Collaboration), preprint CERN-EP/80-187 (1980).
P. Fritze et al. [ABCLOS (BEBC) Collaboration], submitted to Phys. Lett. (1980).

5) D.O. Morrison, preprint CERN-EP/80-190 (1980).

6) L. Maiani, preprint CERN TH.2846 (1980).

7) S. Hama et al., DOE/ER 01545-282 (1980).

8) L. Wolfenstein, Phys. Rev. D 17 (1978) 2369.

9) D. d. Wu, HUTP-80/A032 (1980).

10) N. Cabibbo, Phys. Lett. 72B (1978) 333.

11) J. Blietschau et al., Nucl. Phys. B133 (1978) 205.
N. Armenise et al., preprint CERN-EP/80-225 (1980).

12) S.E. Willis et al., Phys. Rev. Lett. 45 (1980) 522.
S.E. Willis et al., Phys. Rev. Lett. 45 (1980) 1370.

13) A.M. Cnops et al., Phys. Rev. Lett. 40 (1978) 144.
C. Baltay, talk at DESY, June 1980.
USA-Canada-Japan-Korea Collaboration, preprint Fermilab-Conf. 80-92 (1980).

14) A.A. Hahn et al., submitted to Phys. Lett. (1980).

15) P. Miné, Inst. Phys. Conf. Ser. No. 42 (1978) 140.

16) M. Conversi et al., Nucl. Instrum. Methods 151 (1978) 103.

17) W.R. Frisken et al., FNAL experiment E553.

18) P. Allen et al., Nucl. Phys. B176 (1980) 269, 284.

Table 1

Comparison between low-energy and standard ν beams
450 GeV - 10^{13} protons - Target: 3 mm Ø Be - 8 elements 10 cm

		Low-energy beam	Standard WB beam
Detector 100 tons at 17 km			
Total flux (per GeV·m^2)	ν_μ	$2.89 \pm 0.22 \times 10^{7}$	$3.75 \pm 0.22 \times 10^{7}$
Mean energy (GeV)		32.5	41.0
Flux 10-30 GeV (per GeV·m^2)		2.04×10^{7}	1.49×10^{7}
Total No. of events		$3.34 \pm 0.19 \times 10^{-2}$	$5.70 \pm 0.22 \times 10^{-2}$
Mean energy (GeV)		56.6	67.6
Events 10-30 GeV		1.58×10^{-2}	1.12×10^{-2}
Total flux (per GeV·m^2)	ν_e	$2.01 \pm 0.06 \times 10^{5}$	$2.49 \pm 0.05 \times 10^{5}$
Mean energy (GeV)		50.7	59.7
Flux 10-30 GeV (per GeV·m^2)		7.39×10^{4}	6.77×10^{4}
Total No. of events		$3.80 \pm 0.10 \times 10^{-4}$	$5.71 \pm 0.16 \times 10^{-4}$
Mean energy (GeV)		81.7	89.8
Events 10-30 GeV		6.28×10^{-5}	5.34×10^{-5}
Detector 0.32 tons at "BEBC"			
Total flux (per GeV·m^2)	ν_μ	$1.12 \pm 0.03 \times 10^{10}$	$8.84 \pm 0.24 \times 10^{9}$
Mean energy (GeV)		20.9	26.7
Flux 10-30 GeV (per GeV·m^2)		6.75×10^{9}	4.89×10^{9}
Total No. of events		$3.99 \pm 0.07 \times 10^{-2}$	$4.28 \pm 0.07 \times 10^{-2}$
Mean energy (GeV)		45.7	59.9
Events 10-30 GeV		2.13×10^{-2}	1.68×10^{-2}
Total flux (per GeV·m^2)	ν_e	$1.04 \pm 0.02 \times 10^{8}$	$1.13 \pm 0.02 \times 10^{8}$
Mean energy (GeV)		37.7	41.5
Flux 10-30 GeV (per GeV·m^2)		5.02×10^{7}	4.77×10^{7}
Total No. of events		$5.65 \pm 0.09 \times 10^{-4}$	$7.49 \pm 0.14 \times 10^{-4}$
Mean energy (GeV)		62.7	67.9
Events 10-30 GeV		1.35×10^{-4}	1.28×10^{-4}

Figure captions

Fig. 1 : Wide-band neutrino beam line across the profile of the Jura mountain.

Fig. 2 : Neutrino beam spectra at 17 km from the production target.

Fig. 3 : Ratio of ν_μ spectra in detector 1 and detector 2.

Fig. 4 : Exploded view of one module of the electron calorimeter.

Fig. 5 : a) Linearity response as a function of electromagnetic energy.
b) Energy resolution for electromagnetic showers.

Fig. 6 : Test set-up for the flash-tube planes with a photograph of a cosmic-ray track.

Fig. 7 : Efficiency of the flash chambers versus high voltage at two extreme positions along the tubes. The percentage of accidentals is also shown.

Fig. 8 : Schematic view of one dipole magnet, and magnetic field configuration.

Fig. 9 : Momentum resolution for muon tracks.

Fig. 10 : Identification efficiency for muons. The dashed curve refers to quasielastic events only.

Fig. 11 : Trigger efficiency for electrons as a function of the number of radiation lengths traversed.

Fig. 12 : Over-all view of the detector.

Fig. 13 : Examples of simulated events: (a) CC ν_μ; (b) NC; (c) CC ν_e.

Fig. 14 : Examples of quasielastic events: (a) CC ν_μ, and (b) CC ν_e.

Fig. 15 : Sensitivity of the experiment in terms of $\sin^2 2\theta$, Δm^2, together with recent results.

EXTENSION OF THE WIDE-BAND NEUTRINO BEAM

THROUGH THE JURA MOUNTAIN

Longitudinal cross-section

beam path in the air	:	6 210 m.
beam path in the rock	:	10 440 m.
total path	:	16 650 m.

(SPS-Survey group)

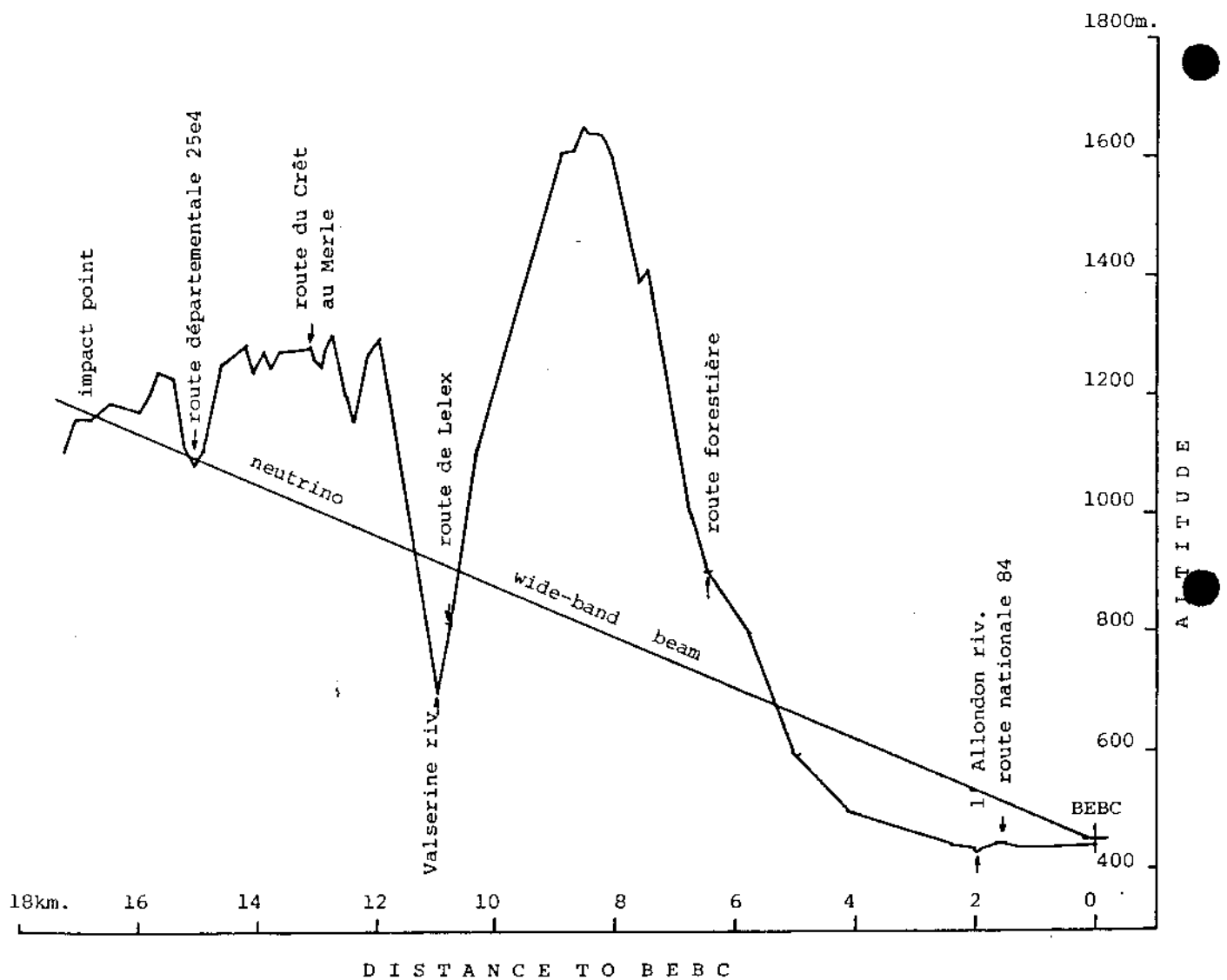

Fig. 1

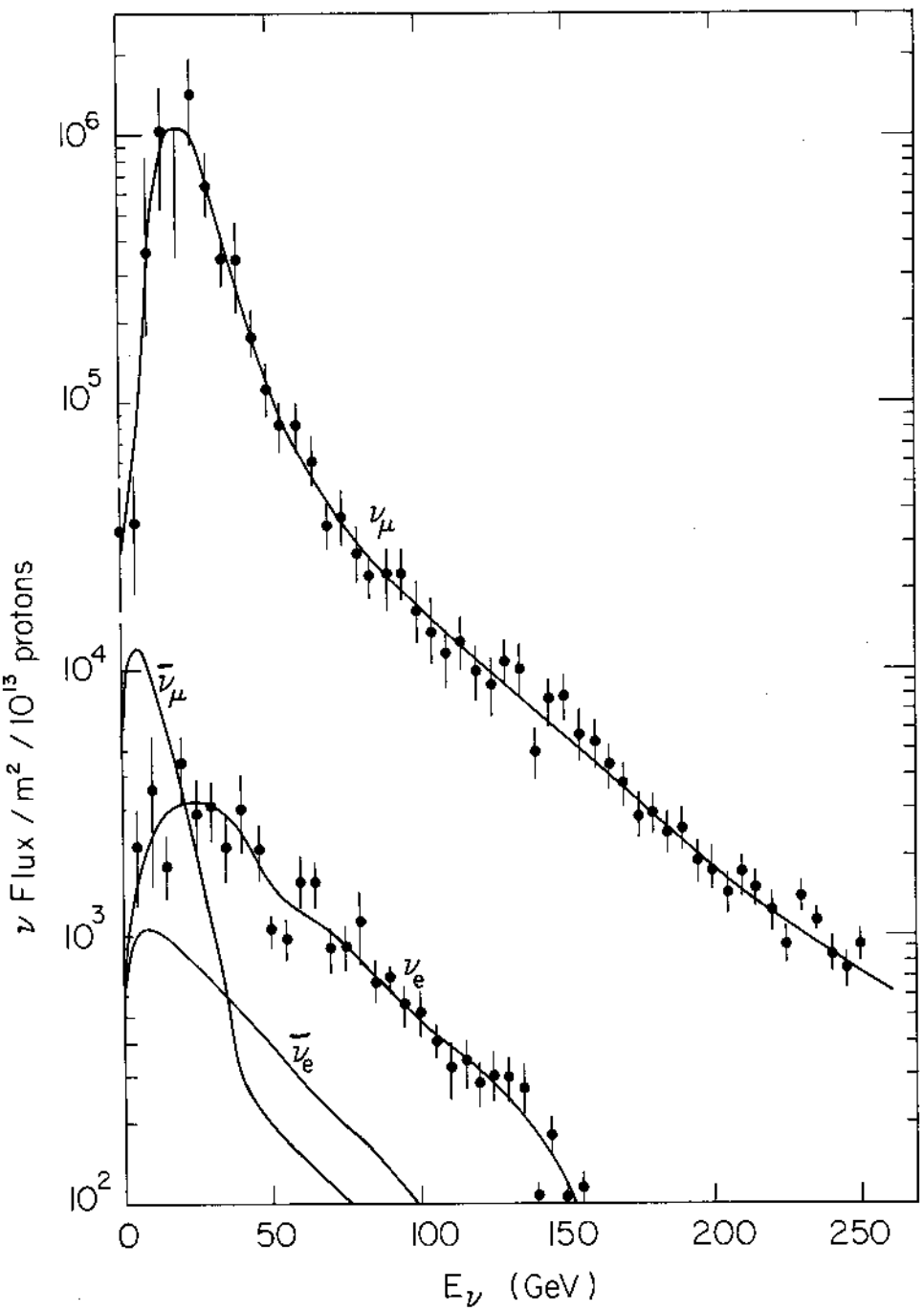
10^6
10^5
10^4
10^3
10^2
ν_μ
$\bar{\nu}_\mu$
ν_e
$\bar{\nu}_e$
ν Flux / m^2 / 10^{13} protons
0
50
100
150
200
250
E_ν (GeV)

Fig. 2

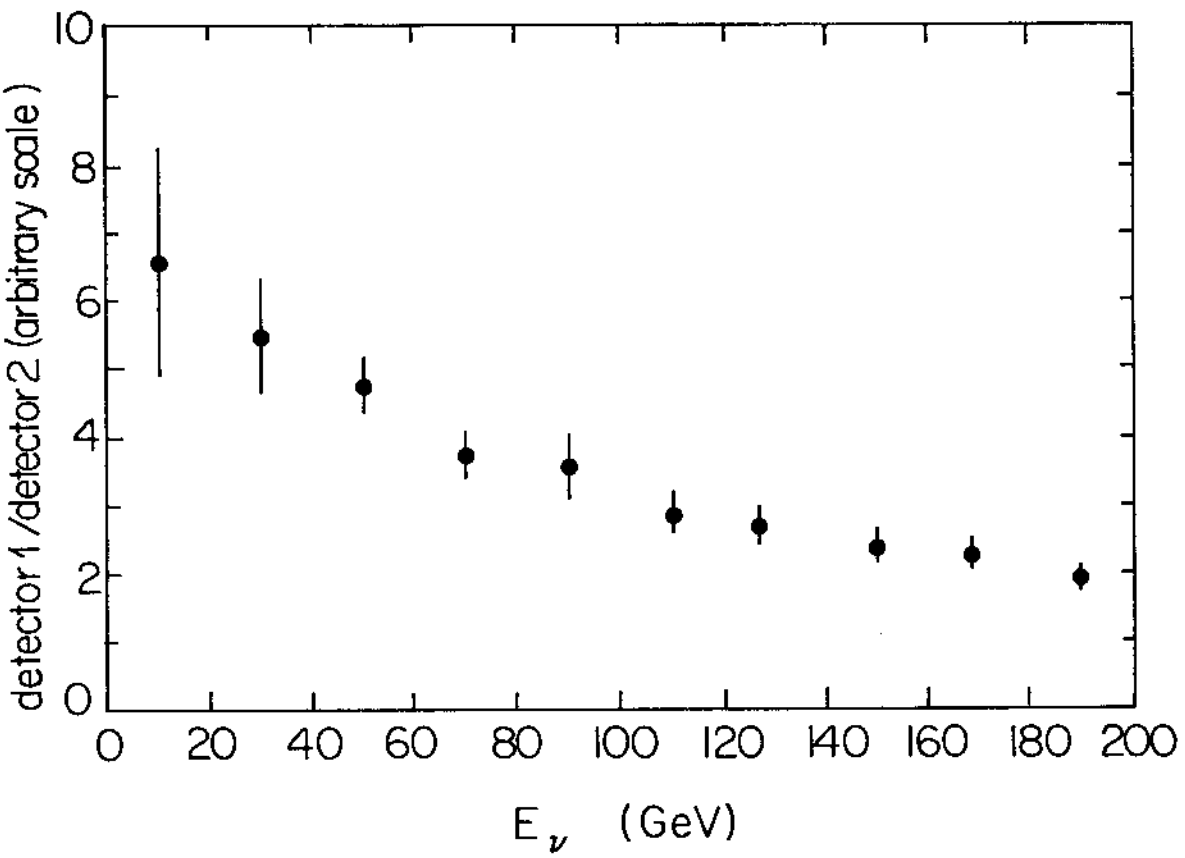
detector 1 /detector 2 (arbitrary scale)
0
2
4
6
8
10
0
20
40
60
80
100
120
140
160
180
200
E_ν (GeV)

Fig. 3

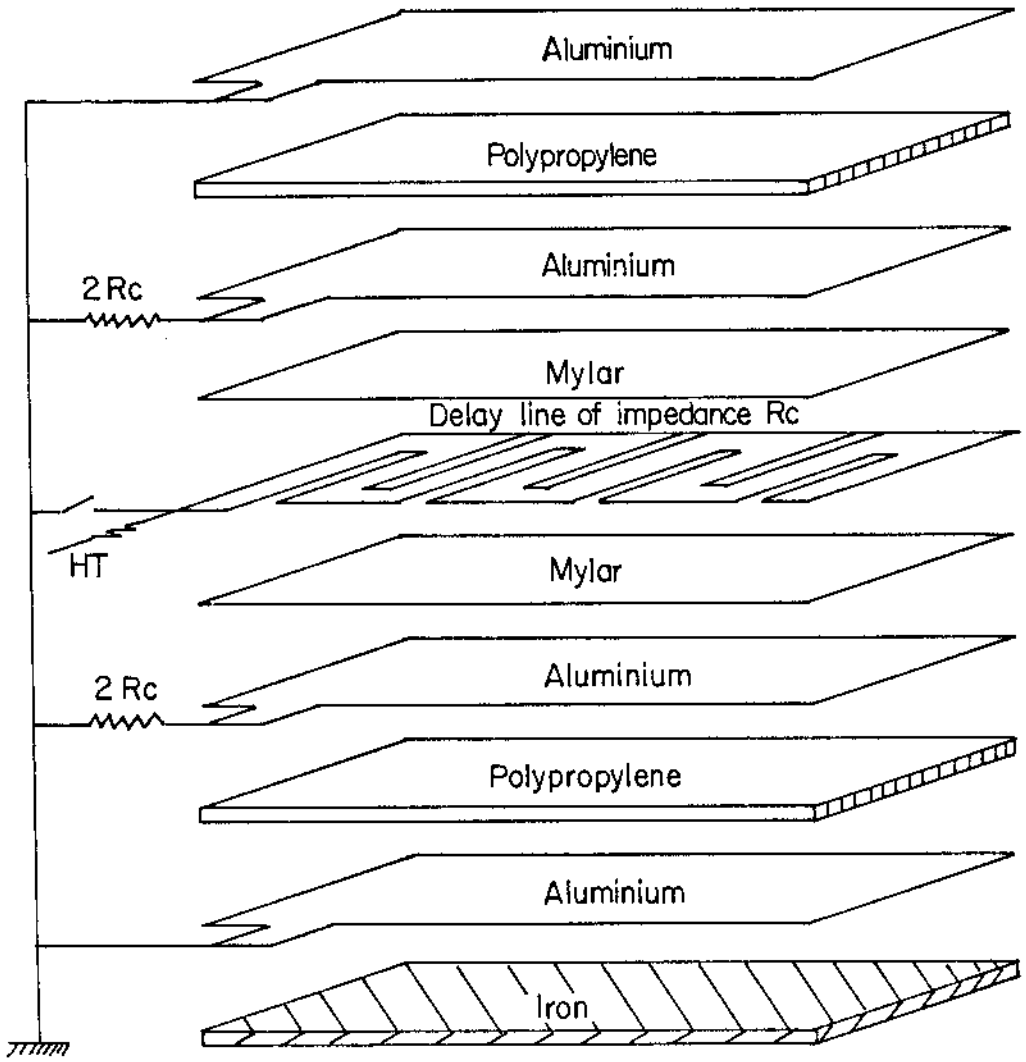
Aluminium
Polypropylene
Aluminium
2 Rc
Mylar
Delay line of impedance Rc
HT
Mylar
Aluminium
2 Rc
Polypropylene
Aluminium
Iron

Fig. 4

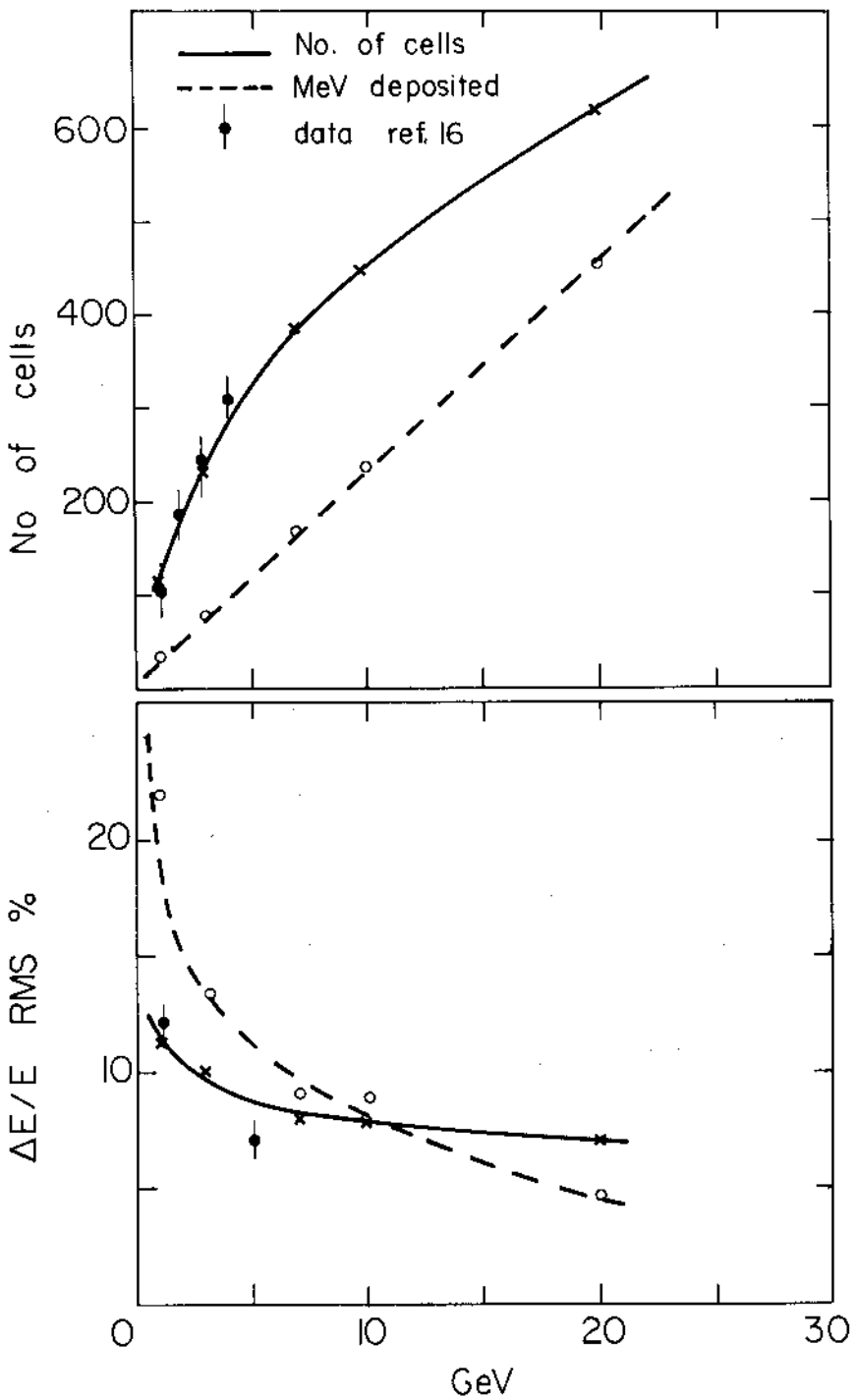
No. of cells
MeV deposited
data ref. 16
600
400
200
No of cells
20
10
ΔE/E RMS %
0
10
20
30
GeV

Fig. 5

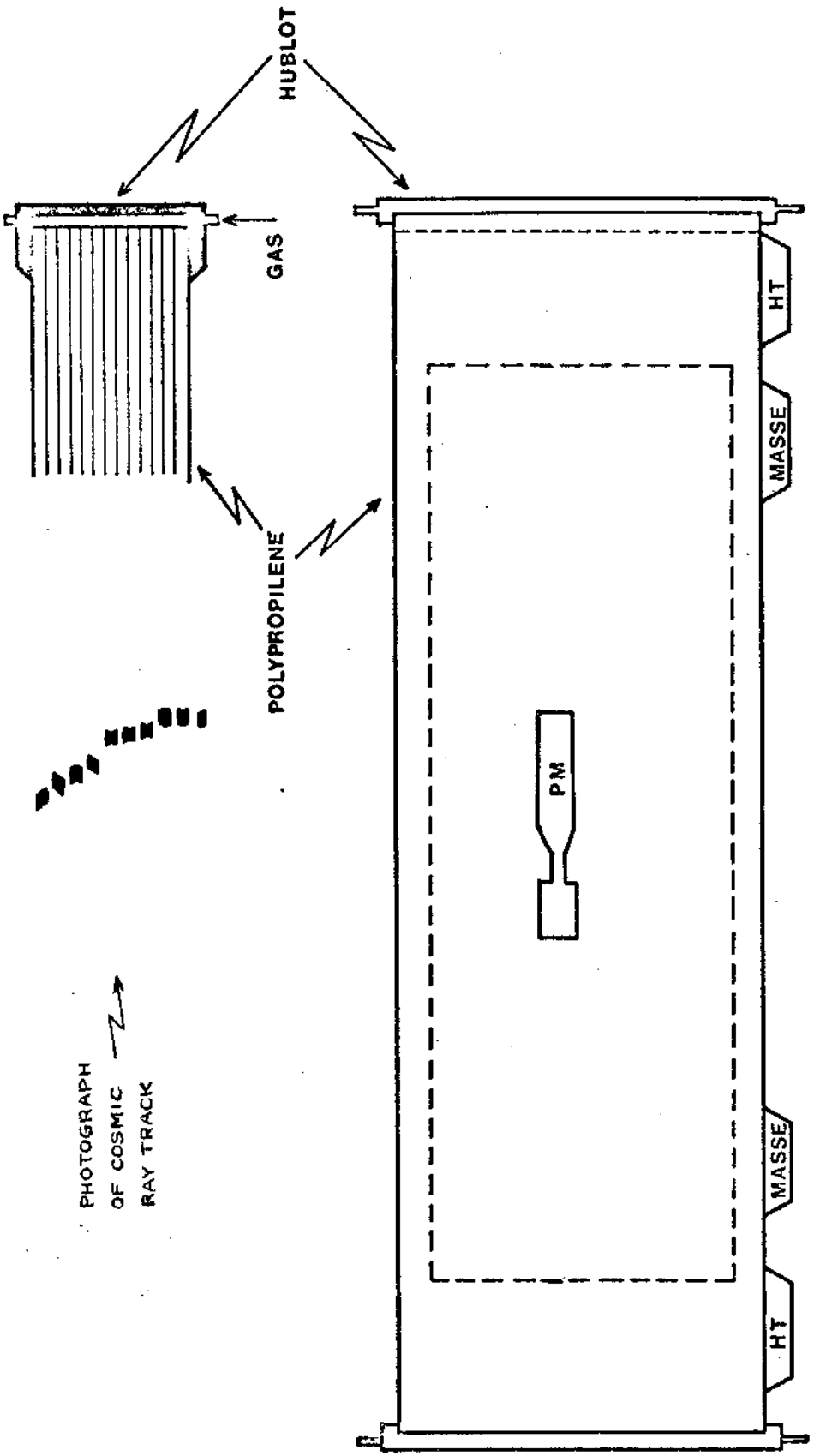
HUBLOT
GAS
POLYPROPILENE
HT
MASSE
PM
MASSE
HT
PHOTOGRAPH
OF COSMIC
RAY TRACK

Fig. 6

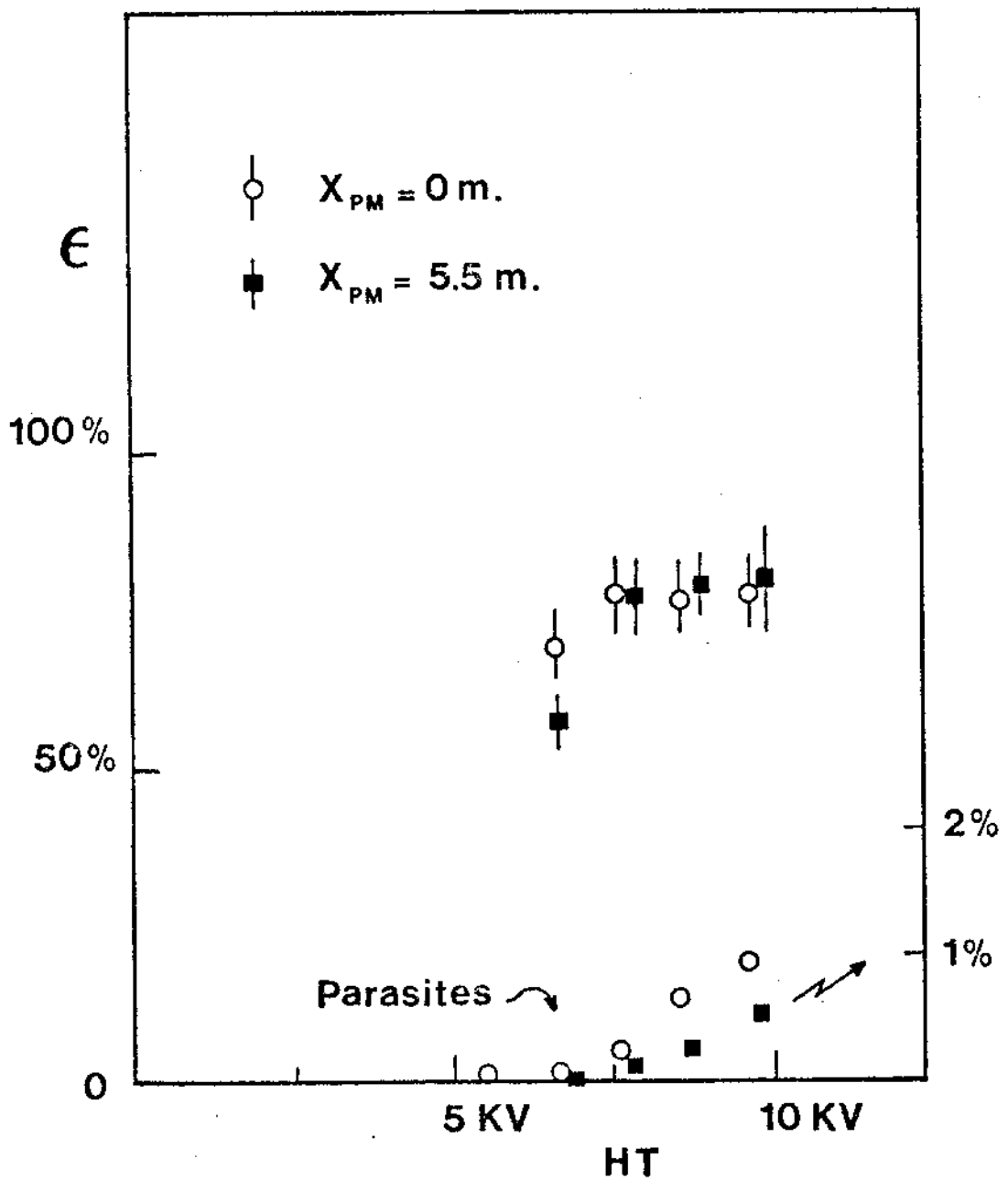

Fig. 7

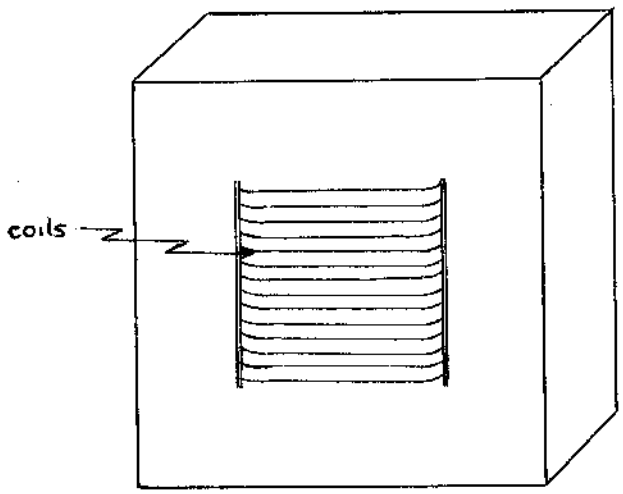

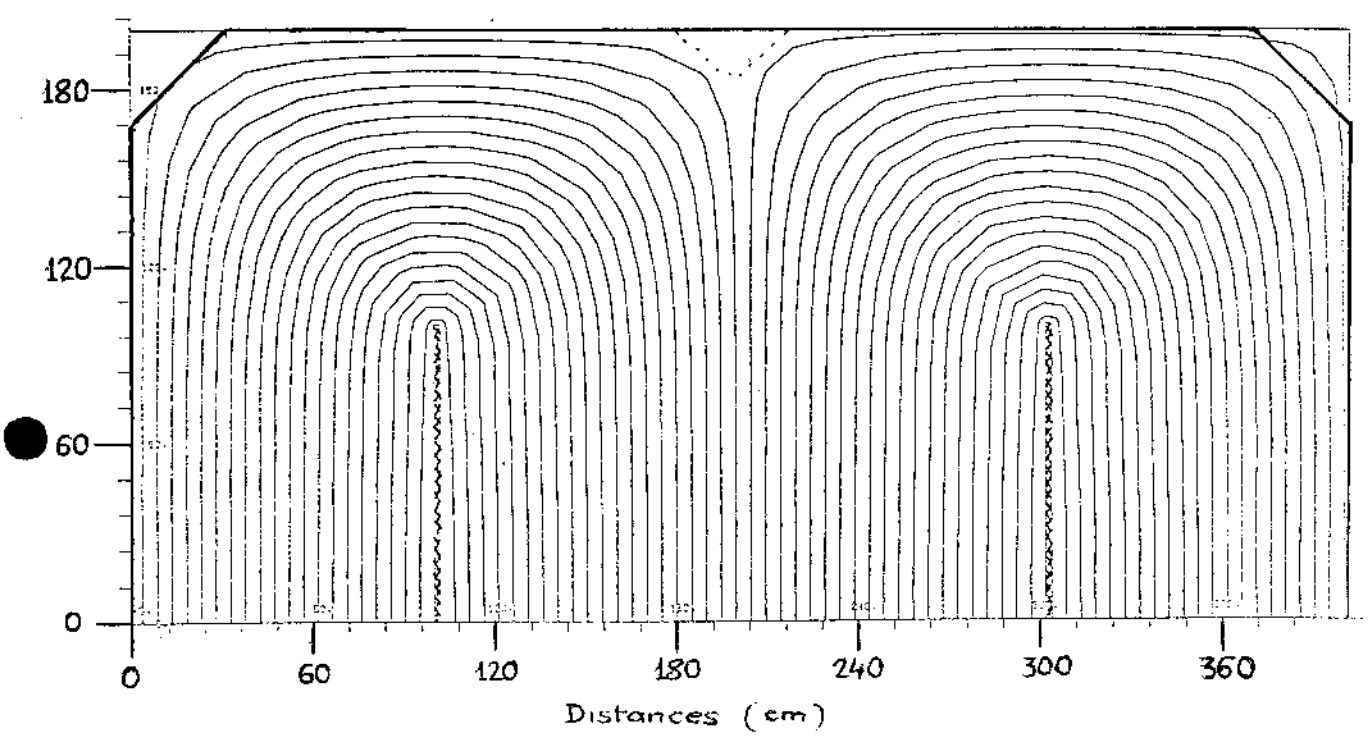

Fig. 8

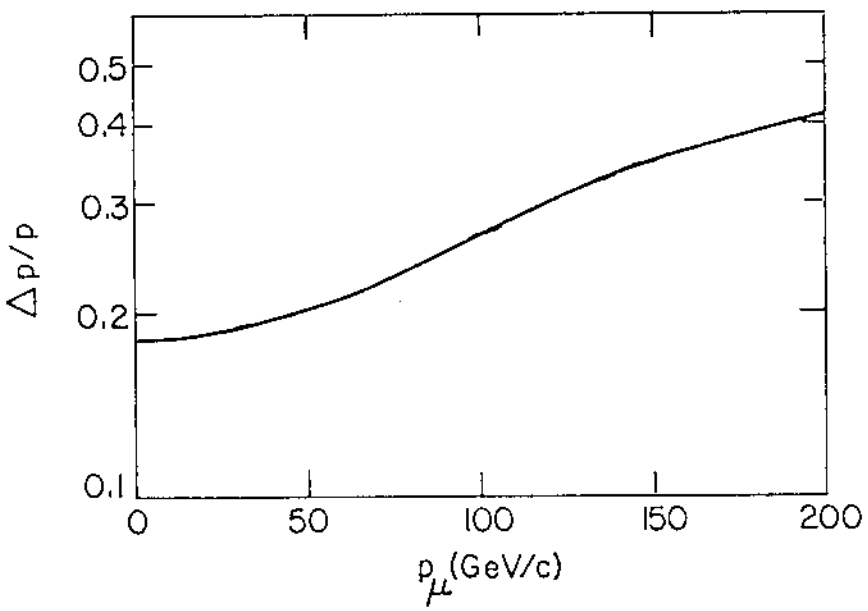

Fig. 9

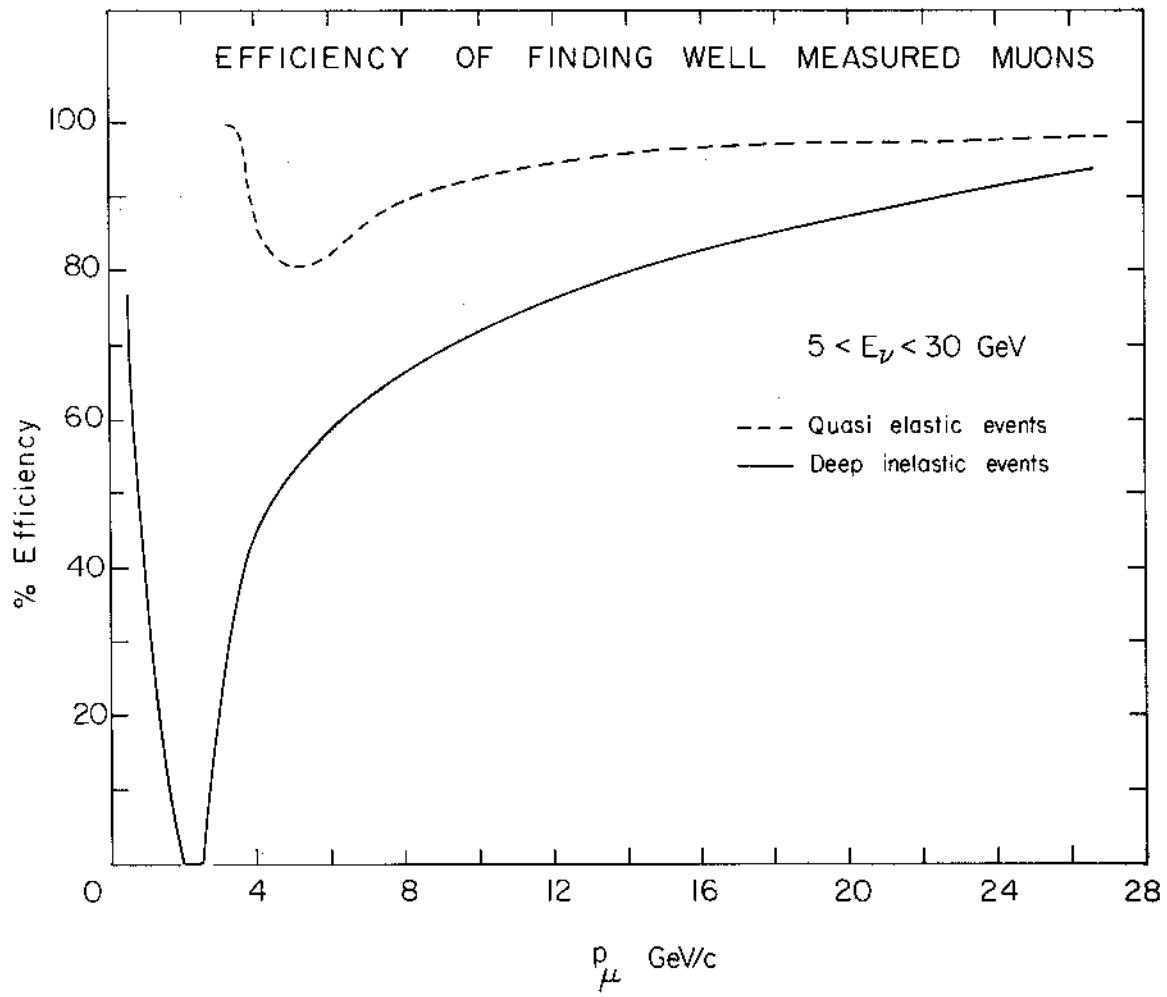
EFFICIENCY OF FINDING WELL MEASURED MUONS
100
80
60
40
20
0
% Efficiency
4
8
12
16
20
24
28
p_μ GeV/c
$5 < E_\nu < 30$ GeV
Quasi elastic events
Deep inelastic events

Fig. 10

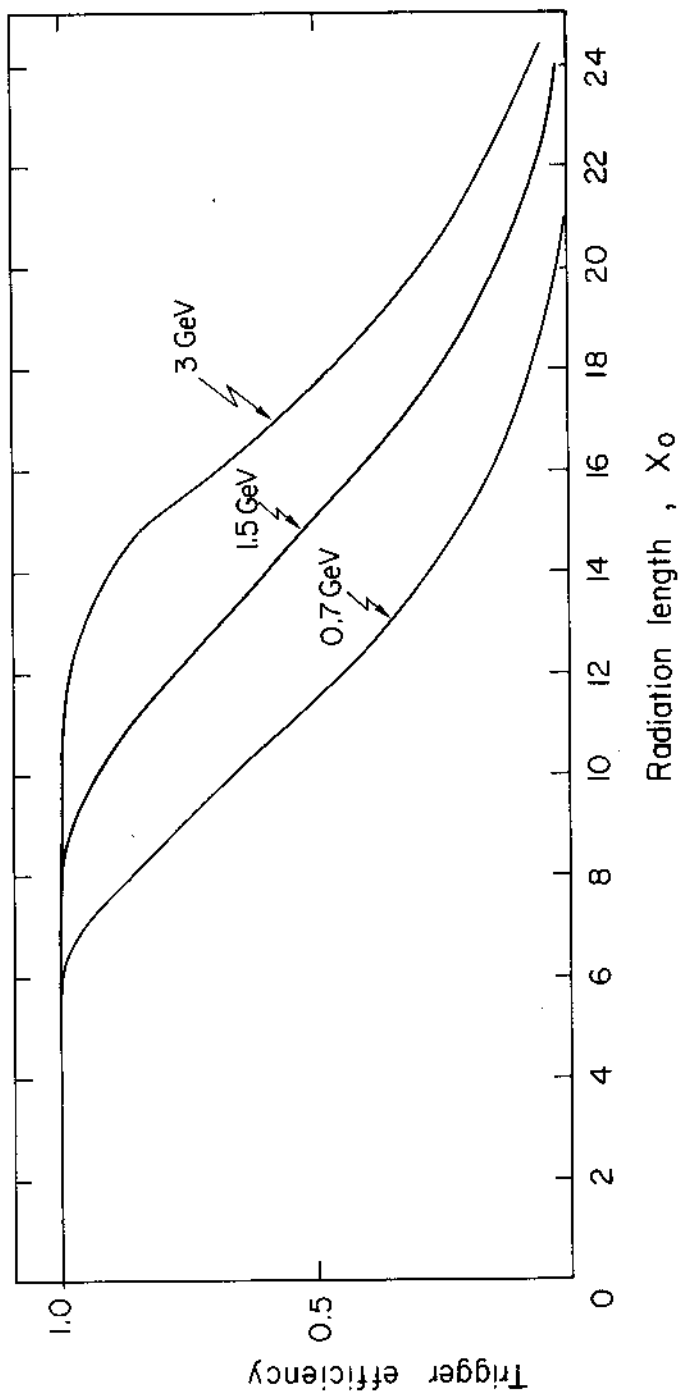
Trigger efficiency
1.0
0.5
0
2
4
6
8
10
12
14
16
18
20
22
24
Radiation length , X_o
3 GeV
1.5 GeV
0.7 GeV

Fig. 11

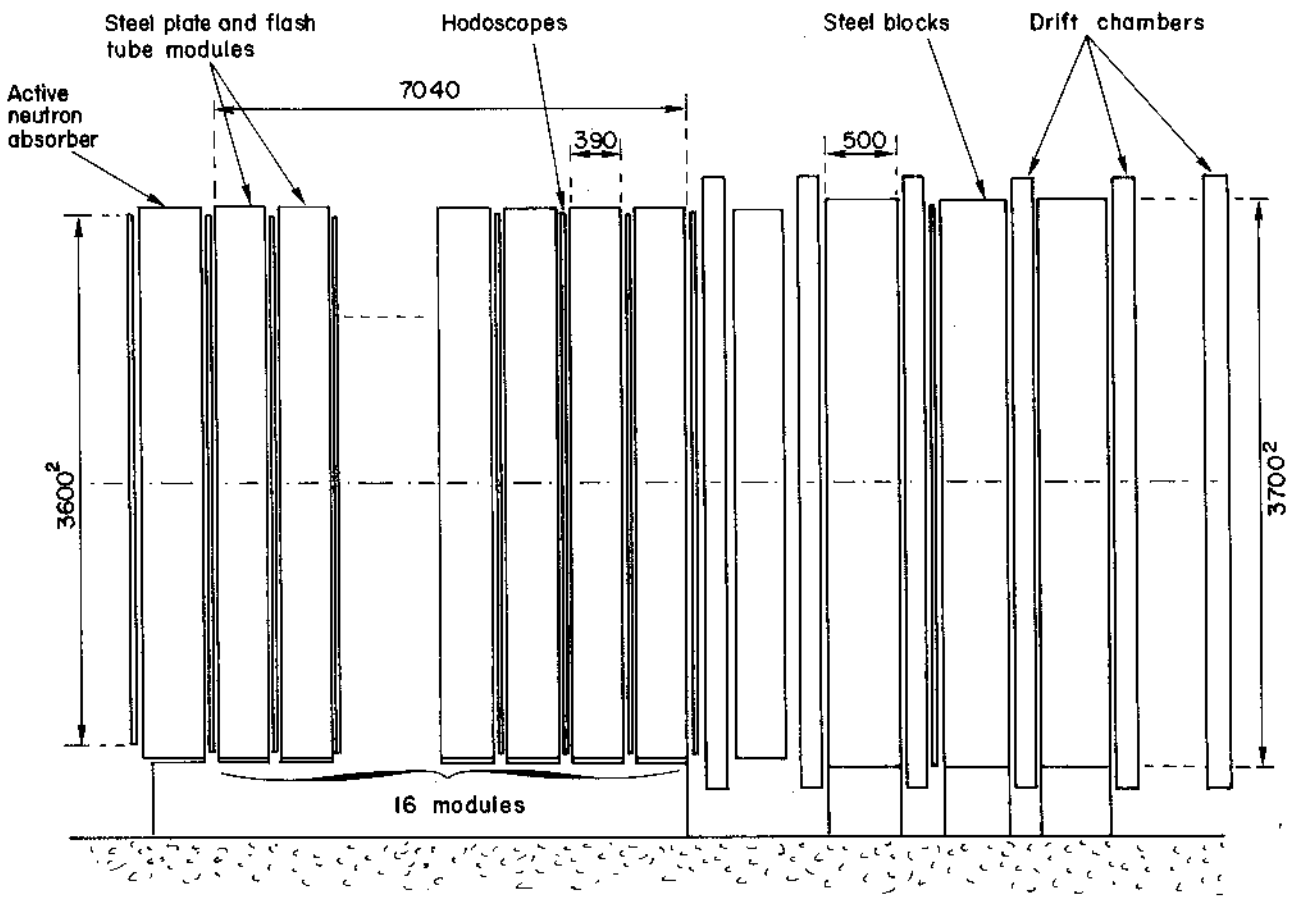
Steel plate and flash tube modules
Hodoscopes
Steel blocks
Drift chambers
Active neutron absorber
7040
390
500
3600²
3700²
16 modules

Fig. 12

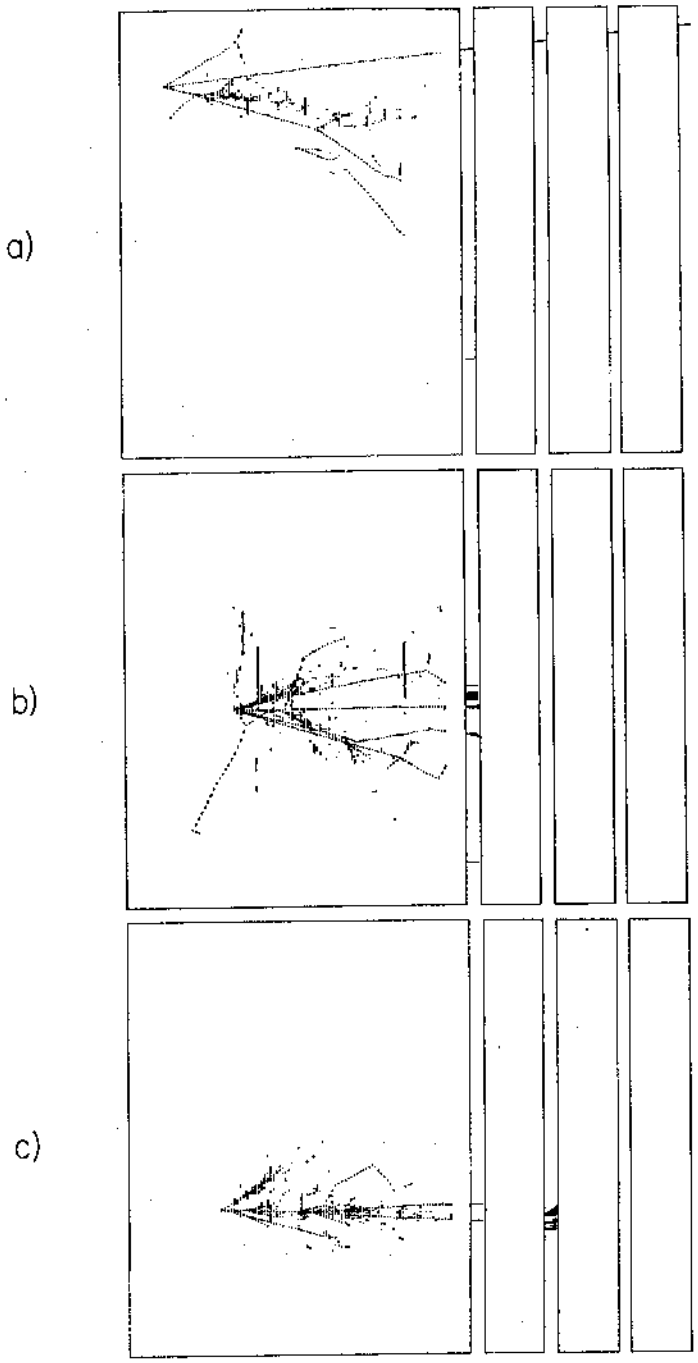

Fig. 13

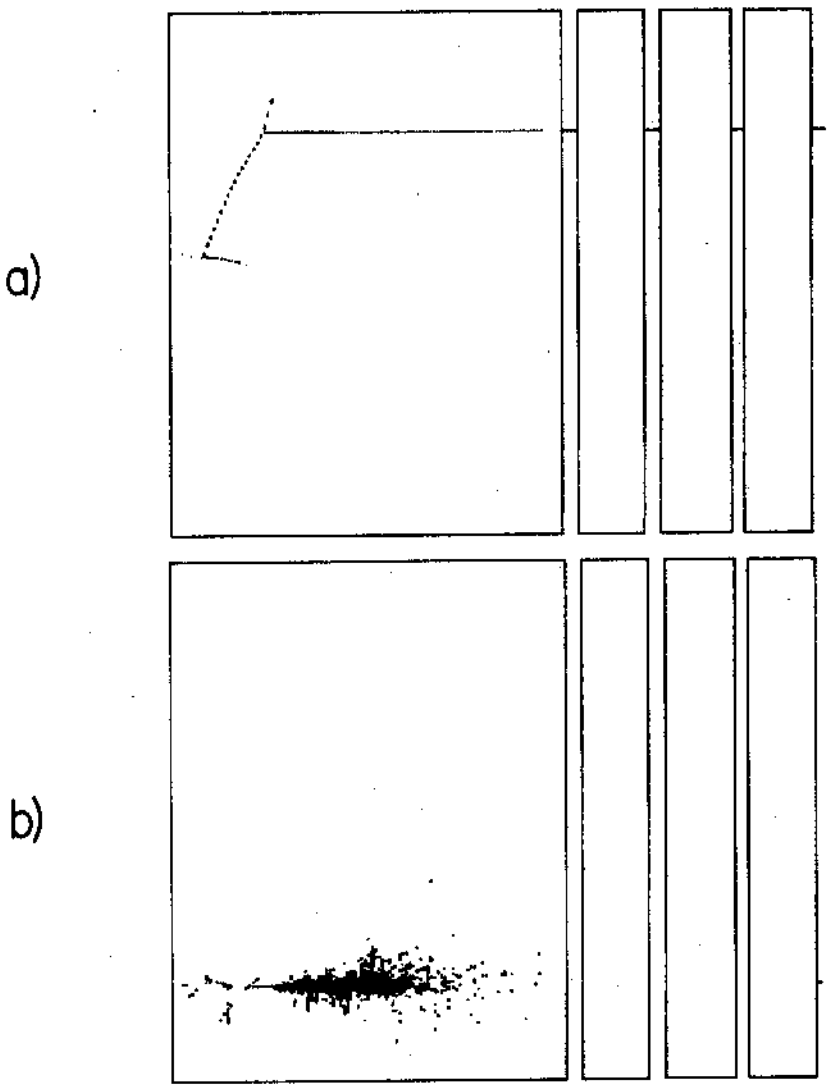

Fig. 14

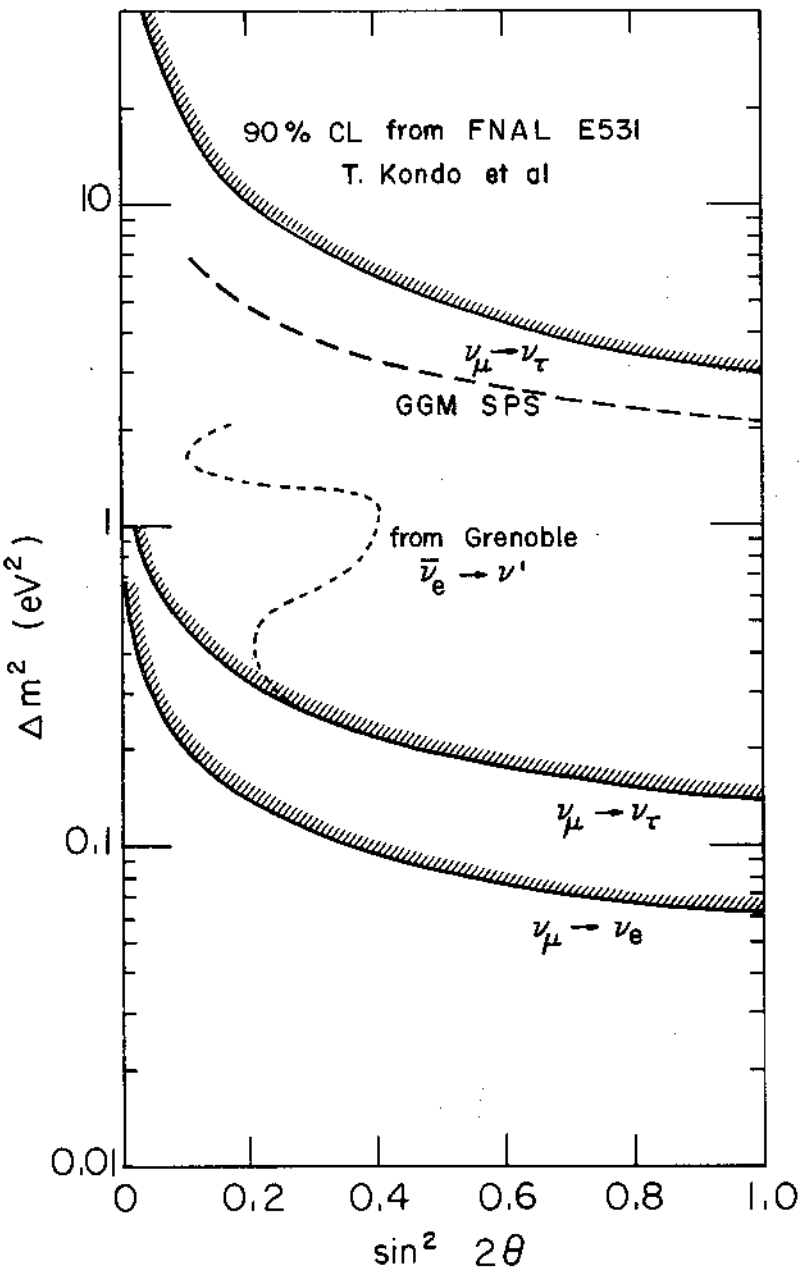
90% CL from FNAL E531
T. Kondo et al
$\nu_\mu \rightarrow \nu_\tau$
GGM SPS
from Grenoble
$\bar{\nu}_e \rightarrow \nu'$
$\nu_\mu \rightarrow \nu_\tau$
$\nu_\mu \rightarrow \nu_e$
10
1
0.1
0.01
Δm^2 (eV^2)
0
0.2
0.4
0.6
0.8
1.0
$\sin^2 2\theta$

Fig. 15

APPENDIX 1

Ref.: SPS-SU/JPQ/sg

Date: 17.09.1980

M E M O R A N D U M

Copy to/Copie à:

To/A : F. VANNUCCI / EP

From/De : J.-P. QUESNEL / SPS-SU

Subject/: Projet extension Neutrino
Objet

L'étude géographique du projet d'extension Neutrino a conduit au résultat suivant.

Le faisceau "sort" de terre en un point situé à environ 130 m à l'Est de la route départementale No 25, au pied d'un talus très facilement accessible.

La précision des résultats peut être estimée à l'ordre de 1 m environ, tant en position altimétrique que planimétrique, ce qui ne peut modifier en rien les conclusions d'une telle étude succincte, vu l'environnement très favorable à l'installation d'un détecteur, qui pourrait même être enterré, si besoin était.

Un accès est facilement réalisable depuis le CD No 25 par un chemin existant déjà d'une part, et par une autre liaison à construire jusqu'à la zone concernée d'autre part (voir plan ci-joint).

Annexes : un plan de situation
un plan de détail

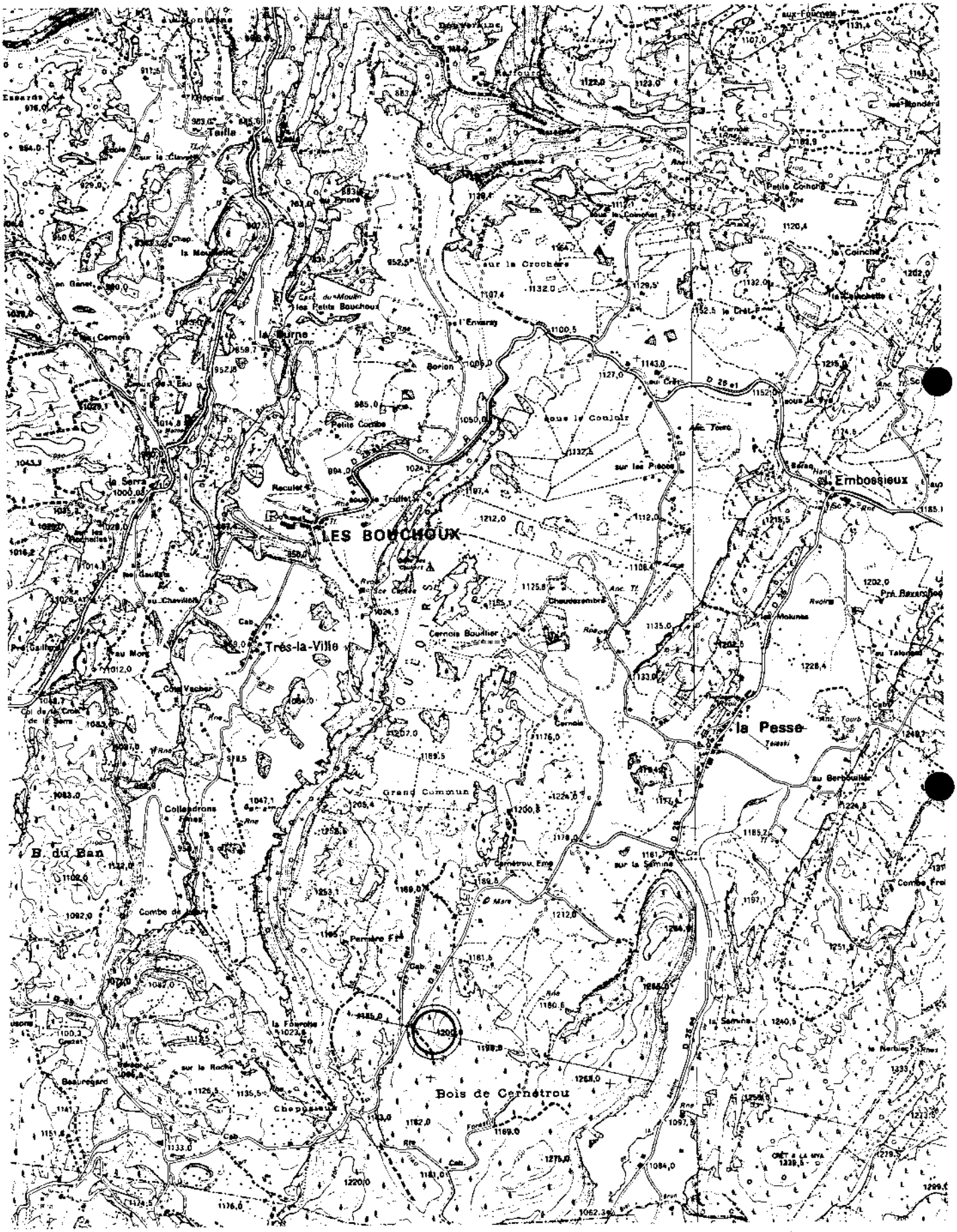

SITUATION : 1 : 25000

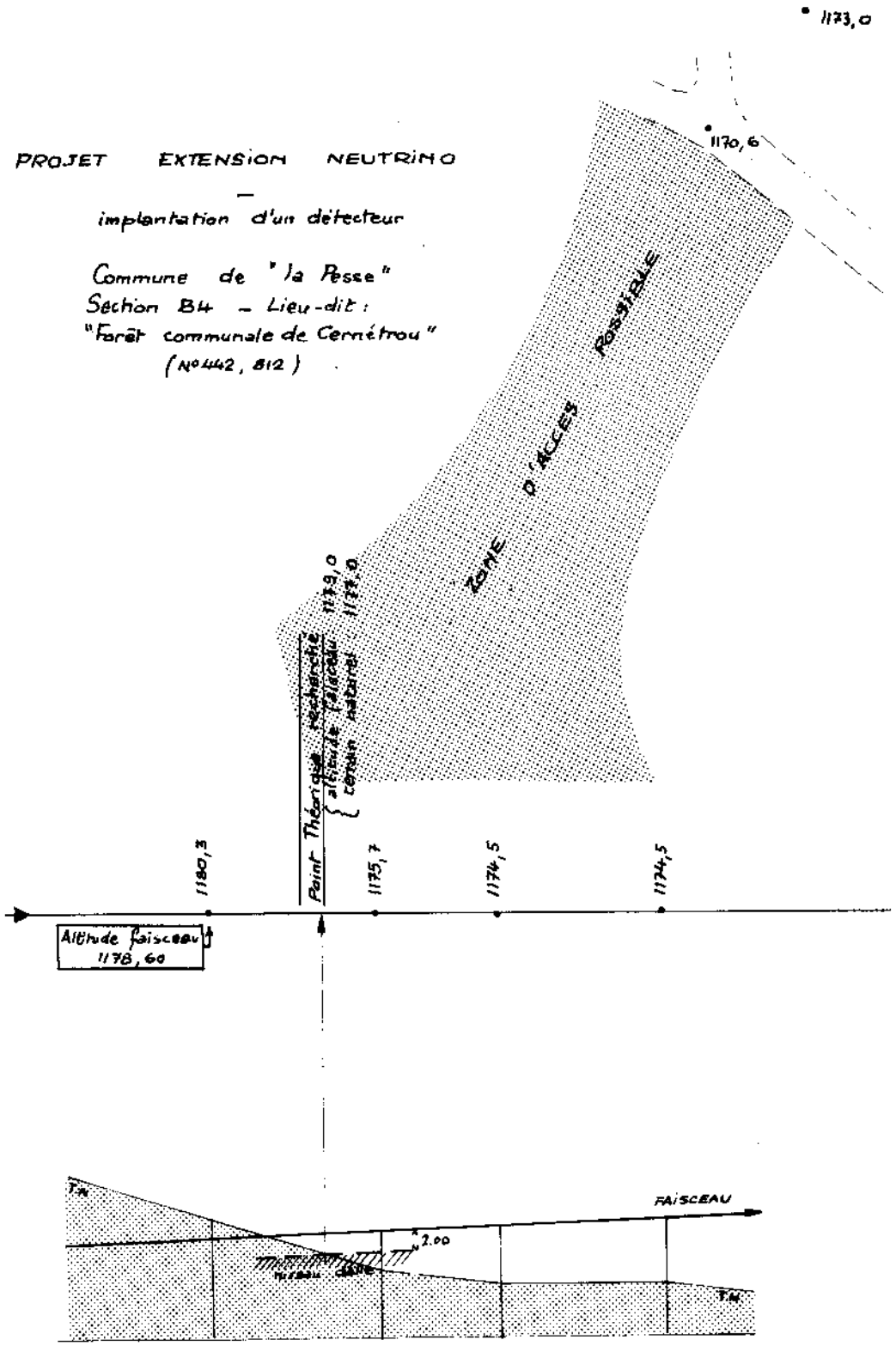
1173,0
1170,6
PROJET EXTENSION NEUTRINO
implantation d'un détecteur
Commune de "la Pesse"
Section B4 - Lieu-dit :
"Forêt communale de Cernétrou"
(N°442, 812)
ZONE D'ACCES POSSIBLE
Point Théorique recherché
altitude faisceau 1179,0
terrain naturel 1177,0
1180,3
1175,7
1174,5
1174,5
Altitude faisceau
1178,60
FAISCEAU
2,00
T.N.
T.N.

APPENDIX 2

ESTIMATE OF COSTS

	MSFr
Housing in the mountain	0.5
Electron calorimeters	
iron + flash-tubes (175 tons)	0.35
pulsing + HT	0.12
read-out (470,000 channels)	0.50
gas system	0.5
manpower	0.35
Muon spectrometers	
iron (reshaping)	0.25
chambers (1000 wires)	0.2
Trigger system	
scintillators (220 m^2)	0.25
tubes (306, 2")	0.15
Electronics	0.20
Computers	0.35
Total	3.7